Uplink Performance Analysis of Base Station Antenna Heights in Dense Cellular Networks

Ziyan Yin*, Jun Li*, Ming Ding†, Fei Song*, and David López-Pérez‡
*The School of Electronic and Optical Engineering,
Nanjing University of Science and Technology, Nanjing 210094
†Data61, CSIRO, Sydney, N.S.W. 2015, Australia
‡Nokia Bell Labs, Dublin 15, Ireland
{ziyan.yin,jun.li,fei.song}@njust.edu.cn, ming.ding@data61.csiro.au, dr.david.lopez@ieee.org

***Abstract*—In this paper, we investigate the impact of the absolute height difference between base station (BS) and user equipment (UE) antennas on the uplink performance of dense small cell networks. We use a path loss model adopted by the 3rd Generation Partnership Project to increase the accuracy of our analysis, where transmissions via both line-of-sight and non-line-of-sight paths are considered. To achieve more practical results, we also consider that UEs are associated with the BS that has the smallest path loss. Based on the performance derived, we then prove that the coverage probability and the area spectral efficiency (ASE) will continuously decrease to zero as the density of BSs grows. To prevent this ASE crash to zero, we also show that reducing the antenna height difference between the BSs and UEs is an effective method. Moreover, our results reveal that the existence of the BS-to-UE antenna height difference changes the optimal operation point of the fractional path loss compensation factor ϵ.**

I. Introduction

With the rapid proliferation of smart user devices, traditional cellular networks have been gradually strained to a breaking point in terms of data provision. In this context, small cell networks (SCNs) have attracted a lot of attention, and are becoming one of the enabling technologies for the next generation of cellular networks [1–3].

In recent years, many studies have been carried out to understand the performance of dense SCNs. Based on stochastic geometry and considering the downlink (DL), small cell base stations (BSs) positions are typically modelled as a Homogeneous Poisson Point Process (HPPP) on the plane [4], and the performance of a typical user equipment (UE) located at the origin is evaluated. A similar approach can be used in the uplink (UL) performance analysis, where both BS and UE positions are also usually modelled as a HPPP [5]. This assumption does not consider that the BS and UE positions are correlated [5, 6], but help us to get closed-form results. Capturing this dependence is not easy [7]. In this paper, we do not consider this dependence and model both BSs and UEs as HPPPs. Similarly and looking at the UL, Sarabjot Singh *et al.* [8] investigated the UL signal to interference plus noise ratio (SINR) and rate coverage using a novel model. However, they did not consider the existence of line-of-sight (LoS) and non-line-of-sight (NLoS) transmissions, and thus they could only apply a user association strategy (UAS), in which each UE is associated with its nearest BS. Tianyang Bai *et al.* [9] analysed the SINR distribution and rate coverage, under LoS and NLoS transmissions, and accounting for different antenna geometries. Ming Ding *et al.* [10] also studied the SINR distribution and rate coverage, under LoS and NLoS transmissions, while additionally considering the antenna height difference between BSs and UEs. Both works lead to interesting conclusions, however, they focused only on the DL. No results are available for the UL, where fractional power control (FPC) for path-loss compensation is in place.

In this paper, we study the UL network performance, e.g., the coverage probability and the area spectral efficiency (ASE), while considering LoS and NLoS transmissions and the antenna height difference between BSs and UEs. Specifically, we first model the distributions of BSs and UEs as HPPPs. Then, we adopt a path loss model used by the 3rd Generation Partnership Project (3GPP), which incorporates probabilistic LoS and NLoS transmissions, to obtain tractable expressions for the coverage probability and the ASE. Finally, we utilise a practical UAS, in which an UE associates with the BS that has the smallest path loss. Simulation results are shown to verify our theoretical analysis.

The main contributions of this paper are as follows:

- We develop the expressions of the coverage probability and the ASE in the UL, considering LoS and NLoS transmissions and the antenna height difference between BSs and UEs;
- We confirm theoretically the existence of *the ASE Crash* in the UL, i.e., the ASE dramatically reduces to zero when λ becomes large enough, and propose an effective method to avoid it, i.e., lowering the BS antenna height straight to the UE antenna height;
- We optimise the FPC path-loss compensation factor ϵ to maximise performance.

II. System Model

We consider an UL cellular network, in which BSs and UEs are modeled as independent HPPPs with densities λ BSs/km^2 and λ^{UE} UEs/km^2, respectively, where $\lambda^{\mathrm{UE}} >> \lambda$, i.e., each BS has in its coverage at least one associated active UE on each time-frequency resource block [9]. We assume that both BSs and UEs are equipped with isotropic antennas, and for the

978-1-5386-4727-1/18/$31.00 ©2018 IEEE

UAS, that each UE is associated with the BS at the smallest path loss.

For the analysis, from all the BSs, we randomly choose one BS denoted as the typical BS, and assume it is located at the origin. The typical UE is the UE associated with the typical BS, and the other UEs using the same time-frequency resource block in neighbouring BSs are denoted as the interferers. The two-dimensional distance (2D) between a BS and a UE is denoted by *r*. Moreover, the BS-to-UE antenna height difference is denoted by *L*. Thus, the three-dimensional (3D) distance can be expressed as

$$\omega = \sqrt{r^2 + L^2}. \tag{1}$$

A. Pass Loss Model

Following [10–12], we first adopt a very general path loss model. In this model, the pass loss $\zeta(\omega)$ is a function of distance ω and is segmented into *N* pieces:

$$\zeta(\omega) = \begin{cases} \zeta_1(\omega), & 0 < \omega \le d_1 \\ \zeta_2(\omega), & d_1 < \omega \le d_2 \\ \vdots & \vdots \\ \zeta_N(\omega), & \omega > d_{N-1} \end{cases}. \tag{2}$$

In (2), each piece $\zeta_n(\omega)$, $n \in \{1, 2, \ldots, N\}$ is modeled as

$$\zeta_n(\omega) = \begin{cases} A_n^{\mathrm{L}} \omega^{\alpha_n^{\mathrm{L}}}, & \mathrm{LoS} : P_{r_n}^{\mathrm{L}}(\omega) \\ A_n^{\mathrm{NL}} \omega^{\alpha_n^{\mathrm{NL}}}, & \mathrm{NLoS} : \left(1 - P_{r_n}^{\mathrm{L}}(\omega)\right) \end{cases}, \tag{3}$$

where A_n^{L} (A_n^{NL}) is the pass loss at a reference distance $\omega = 1$ for the LoS (NLoS) case, and α_n^{L} (α_n^{NL}) is the pass loss exponent for the LoS (NLoS) case. Moreover, $P_{r_n}^{\mathrm{L}}(\omega)$ is the probability that the link between the typical BS and the typical UE is LoS.

In this paper, we consider a path loss function adopted by the 3GPP, as a special case. In more detail, $\zeta(\omega)$ has only one segment, and is modeled as:

$$\zeta(\omega) = \begin{cases} A^{\mathrm{L}} \omega^{\alpha^{\mathrm{L}}}, & \mathrm{LoS} : P_r^{\mathrm{L}}(\omega) \\ A^{\mathrm{NL}} \omega^{\alpha^{\mathrm{NL}}}, & \mathrm{NLoS} : (1 - P_r^{\mathrm{L}}(\omega)) \end{cases}. \tag{4}$$

Correspondingly, the $Pr^{\mathrm{L}}(\omega)$ is modeled as:

$$P_r^{\mathrm{L}}(\omega) = \begin{cases} 1 - \frac{\omega}{d_1}, & 0 < \omega \le d_1 \\ 0, & \omega > d_1 \end{cases}, \tag{5}$$

where d_1 is the largest distance that a LoS link can have.

Note that this special path loss model can be readily extended to more general models, and that we will only use this 3GPP special case in our discussions hereafter.

B. Transmit Power

Different from the DL, the transmit signal power of UE *k* in the UL is a function of the BS-to-UE distance, and is denoted as P_k^t:

$$P_k^t = P_0 \zeta(\omega)^{\epsilon}, \tag{6}$$

where P_0 is the baseline power, and $\epsilon \in (0, 1]$ is the FPC factor.

C. Received Power

Based on (6), the received signal power at the typical BS can be written as

$$P^{\mathrm{rec}} = P_0 \zeta(\omega)^{(\epsilon - 1)} g, \tag{7}$$

where *g* is an independently identical distributed Rayleigh fading random variable, which follows an exponential distribution with the mean of one.

III. Analysis Based on the 3GPP Spacial Case

The coverage probability in the UL for the typical BS and the typical UE can be formulated as

$$P^{\mathrm{cov}}(\lambda, T) = \Pr\left[\mathrm{SINR} > T\right], \tag{8}$$

where *T* is the SINR threshold, and the SINR is calculated as

$$\mathrm{SINR} = \frac{P^{\mathrm{rec}}}{\sigma^2 + I_Z}. \tag{9}$$

In (9), P^{rec} is the received signal power, σ^2 is the noise power, Z is the set of interferers, and I_Z is the interference given by

$$I_Z = \sum_Z P_0 \zeta(\omega_z)^{\epsilon} \zeta(\omega_{D_z})^{-1} g_z, \tag{10}$$

where ω_z is the 3D distance of interferer $z \in Z$ to its serving BS, and ω_{D_z} is the 3D distance of interferer $z \in Z$ to the typical BS, and g_z is the channel gain of the multi-path fading channel of interferer $z \in Z$. Since $\omega_{D_z} >> \omega_z$, we can use the distance from the serving BS of interferer z to the typical BS to represent ω_{D_z}.

Based on the proposed path loss and the proposed UAS, we can calculate $P^{\mathrm{cov}}(\lambda, T)$, and present it in Theorem 1.

Theorem 1: $P^{\mathrm{cov}}(\lambda, T)$ can be derived as

$$P^{\mathrm{cov}}(\lambda, T) = \sum_{n=1}^{N} \left(T_n^{\mathrm{L}} + T_n^{\mathrm{NL}}\right). \tag{11}$$

Proof: We omit the proof of this theorem and those of the following three lemmas due to the page limit. We will provide the full proof in the journal version of this work.

In (11), T_n^{L} and T_n^{NL} denote the coverage probability when the typical UE is associated with the typical BS with a LoS and a NLoS link, respectively. Based on the special case treated in this paper, we adopt $N = 2$. In order to investigate the results of T_1^{L}, T_1^{NL}, T_2^{L} and T_2^{NL}, we need to derive the probability density function (PDF) of ω_z.

The PDF of ω_z based on the different cases treated in this paper can be written as follows:

Case 1: When the interference path is LoS, $f_{\omega_z}^{1\mathrm{L}}(u)$ can be derived as

$$f_{\omega_z}^{1\mathrm{L}}(u) = \begin{cases} f_{\omega_z,1}^{\mathrm{L}}(u), & \mathrm{LoS}, \quad 0 < u \le x \\ f_{\omega_z,1}^{1\mathrm{NL}}(u), & \mathrm{NLoS}, \quad 0 < u \le x_1 \end{cases}, \tag{12}$$

where $0 < x \le D$, $D = \sqrt{{d_1}^2 - L^2}$, and

$$x_1 = \sqrt{\left(\frac{A^{\mathrm{L}}}{A^{\mathrm{NL}}}(x^2 + L^2)^{\frac{\alpha^{\mathrm{L}}}{2}}\right)^{\frac{2}{\alpha^{\mathrm{NL}}}} - L^2}. \tag{13}$$

Case 2: When the interference path is NLoS and $x \le D$, $f_{\omega_z}^{\text{1NL}}(u)$ can be derived as

$$f_{\omega_z}^{\text{1NL}}(u) = \begin{cases} \begin{cases} f_{\omega_z,1}^{\text{L}}(u), & \text{LoS}, \quad 0 < u \le x_2, \\ f_{\omega_z,1}^{\text{1NL}}(u), & \text{NLoS}, \quad 0 < u \le x, \end{cases} & r_1 < x \le y_1 \\ \begin{cases} f_{\omega_z,1}^{\text{L}}(u), & \text{LoS}, \quad 0 < u \le D \\ f_{\omega_z,1}^{\text{1NL}}(u), & \text{NLoS}, \quad 0 < u \le y_1 \\ f_{\omega_z,1}^{\text{2NL}}(u), & \text{NLoS}, \quad y_1 < u \le x \end{cases} & y_1 < x \le D \end{cases} \tag{14}$$

where

$$y_1 = \sqrt{\left(\frac{A^{\text{L}}}{A^{\text{NL}}} {d_1}^{\alpha^{\text{L}}}\right)^{\frac{2}{\alpha^{\text{NL}}}} - L^2}, \tag{15}$$

and

$$x_2 = \sqrt{\left(\frac{A^{\text{NL}}}{A^{\text{L}}}(x^2+L^2)^{\frac{\alpha^{\text{NL}}}{2}}\right)^{\frac{2}{\alpha^{\text{L}}}} - L^2}. \tag{16}$$

Case 3: When the interference path is NLoS and $x > D$, $f_{\omega_z}^{\text{2NL}}(u)$ can be derived as

$$f_{\omega_z}^{\text{2NL}}(u) = \begin{cases} f_{\omega_z,1}^{\text{L}}(u), & \text{LoS}, \quad 0 < u \le D \\ f_{\omega_z,1}^{\text{1NL}}(u), & \text{NLoS}, \quad 0 < u \le y_1 \\ f_{\omega_z,1}^{\text{2NL}}(u), & \text{NLoS}, \quad y_1 < u \le D \\ f_{\omega_z,2}^{\text{NL}}(u), & \text{NLoS}, \quad D < u \le x \end{cases}. \tag{17}$$

Specifically,

$$f_{\omega_z,1}^{\text{L}}(u) = \left(1 - \frac{\sqrt{u^2+L^2}}{d_1}\right) 2\pi u\lambda \times \exp\left(-\pi\lambda u^2 + 2\pi\lambda\left(\frac{\left(u^2+L^2\right)^{\frac{3}{2}}}{3d_1} - \frac{\left({u_1}^2+L^2\right)^{\frac{3}{2}}}{3d_1}\right)\right), \tag{18}$$

$$f_{\omega_z,1}^{\text{1NL}}(u) = \frac{\sqrt{u^2+L^2}}{d_1} 2\pi u\lambda \times \exp\left(-\pi\lambda {u_2}^2 + 2\pi\lambda\left(\frac{\left({u_2}^2+L^2\right)^{\frac{3}{2}}}{3d_1} - \frac{\left(u^2+L^2\right)^{\frac{3}{2}}}{3d_1}\right)\right), \tag{19}$$

$$f_{\omega_z,1}^{\text{2NL}}(u) = \frac{\sqrt{u^2+L^2}}{d_1} 2\pi u\lambda \times \exp\left(-\pi\lambda {d_1}^2 + 2\pi\lambda\left(\frac{{d_1}^3}{3d_1} - \frac{\left(u^2+L^2\right)^{\frac{3}{2}}}{3d_1}\right)\right), \tag{20}$$

and

$$f_{\omega_z,2}^{\text{NL}}(u) = \exp\left(-\pi\lambda u^2\right) 2\pi u\lambda, \tag{21}$$

where

$$u_1 = \sqrt{\left(\frac{A^{\text{L}}}{A^{\text{NL}}}(u^2+L^2)^{\frac{\alpha^{\text{L}}}{2}}\right)^{\frac{2}{\alpha^{\text{NL}}}} - L^2}, \tag{22}$$

$$u_2 = \sqrt{\left(\frac{A^{\text{NL}}}{A^{\text{L}}}(u^2+L^2)^{\frac{\alpha^{\text{NL}}}{2}}\right)^{\frac{2}{\alpha^{\text{L}}}} - L^2}. \tag{23}$$

Note that $f_{\omega_z,1}^{\text{L}}(r)$, $f_{\omega_z,1}^{\text{1NL}}(r)$, $f_{\omega_z,1}^{\text{2NL}}(r)$ and $f_{\omega_z,2}^{\text{NL}}(r)$ have the same form as the previous formulas, and use r, r_1, r_2 instead of u, u_1, u_2, respectively.

A. The Result of T_1^{L}

The result of T_1^{L} is the coverage probability when the typical UE is associated with the typical BS with a LoS link of distance less than D.

Lemma 1: T_1^{L} can be computed by

$$T_1^{\text{L}} = \int_0^D \exp\left(-\frac{T\sigma^2}{P_0(A^{\text{L}}\sqrt{r^2+L^2}^{\alpha^{\text{L}}})^{(\epsilon-1)}}\right) \times \mathcal{L}_{I_Z}\left(\frac{T}{P_0(A^{\text{L}}\sqrt{r^2+L^2}^{\alpha^{\text{L}}})^{(\epsilon-1)}}\right) f_{\omega_z,1}^{\text{L}}(r)\mathrm{d}r, \tag{24}$$

and the Laplace transform $\mathcal{L}_{I_Z}(s)$ is expressed as

$$\begin{aligned} \mathcal{L}_{I_Z}(s) = \exp\Bigg\{ & -2\pi\lambda \int_r^D \left(1 - \frac{\sqrt{x^2+L^2}}{d_1}\right) \\ & \times \int_0^\infty \left(f(u,x) f_{\omega_z}^{\text{1L}}(u)\,\mathrm{d}u\,|\text{LoS}\right) x\mathrm{d}x \Bigg\} \\ & \times \exp\Bigg\{ -2\pi\lambda \int_{r_1}^D \frac{\sqrt{x^2+L^2}}{d_1} \\ & \times \int_0^\infty \left(f(u,x) f_{\omega_z}^{\text{1NL}}(u)\,\mathrm{d}u\,|\text{NLoS}\right) x\mathrm{d}x \Bigg\} \\ & \times \exp\Bigg\{ -2\pi\lambda \int_{r_1}^D 1 \\ & \times \int_0^\infty \left(f(u,x) f_{\omega_z}^{\text{2NL}}(u)\,\mathrm{d}u\,|\text{NLoS}\right) x\mathrm{d}x \Bigg\}, \end{aligned} \tag{25}$$

where

$$f(u,x) = \frac{1}{1 + s^{-1}P_0^{-1}\zeta\left(\sqrt{u^2+L^2}\right)^{-\epsilon}\zeta\left(\sqrt{x^2+L^2}\right)}. \tag{26}$$

B. The Result of T_1^{NL}

The result of T_1^{NL} is the coverage probability when the typical UE is associated with the typical BS with an NLoS link of distance less than D.

Lemma 2: T_1^{NL} can be derived as

$$T_1{}^{\text{NL}} = \int_0^D \exp\left(-\frac{T\sigma^2}{P_0(A^{\text{NL}}\sqrt{r^2+L^2}^{\alpha^{\text{NL}}})^{(\epsilon-1)}}\right) \times \mathcal{L}_{I_Z}\left(\frac{T}{P_0(A^{\text{NL}}\sqrt{r^2+L^2}^{\alpha^{\text{NL}}})^{(\epsilon-1)}}\right) f_{\omega,1}^{\text{NL}}(r)\mathrm{d}r, \tag{27}$$

where

$$f_{\omega,1}^{\text{NL}}(r) = \begin{cases} f_{\omega_z,1}^{\text{1NL}}(r), & 0 < r \le y_1 \\ f_{\omega_z,1}^{\text{2NL}}(r), & y_1 < r \le D \end{cases}, \tag{28}$$

and the Laplace transform $\mathcal{L}_{I_Z}(s)$ *for* $0 < r \leq y_1$ *and* $y_1 < r \leq D$ *are respectively expressed as*

$$\begin{aligned}\mathcal{L}_{I_Z}(s) = &\exp\left\{-2\pi\lambda\int_{r_2}^{D}\left(1-\frac{\sqrt{x^2+L^2}}{d_1}\right)\right.\\ &\left.\times\int_0^{\infty}\left(f(u,x)f_{\omega_z}^{1\mathrm{L}}(u)\,\mathrm{d}u\,|\mathrm{LoS}\right)x\mathrm{d}x\right\}\\ &\times\exp\left\{-2\pi\lambda\int_{r}^{D}\frac{\sqrt{x^2+L^2}}{d_1}\right.\\ &\left.\times\int_0^{\infty}\left(f(u,x)f_{\omega_z}^{1\mathrm{NL}}(u)\,\mathrm{d}u\,|\mathrm{NLoS}\right)x\mathrm{d}x\right\}\\ &\times\exp\left\{-2\pi\lambda\int_{D}^{\infty}1\right.\\ &\left.\times\int_0^{\infty}\left(f(u,x)f_{\omega_z}^{2\mathrm{NL}}(u)\,\mathrm{d}u\,|\mathrm{NLoS}\right)x\mathrm{d}x\right\},\end{aligned} \tag{29}$$

and

$$\begin{aligned}\mathcal{L}_{I_Z}(s) = &\exp\left\{-2\pi\lambda\int_{r}^{D}\frac{\sqrt{x^2+L^2}}{d_1}\right.\\ &\left.\times\int_0^{\infty}\left(f(u,x)f_{\omega_z}^{1\mathrm{NL}}(u)\,\mathrm{d}u\,|\mathrm{NLoS}\right)x\mathrm{d}x\right\}\\ &\times\exp\left\{-2\pi\lambda\int_{D}^{\infty}1\right.\\ &\left.\times\int_0^{\infty}\left(f(u,x)f_{\omega_z}^{2\mathrm{NL}}(u)\,\mathrm{d}u\,|\mathrm{NLoS}\right)x\mathrm{d}x\right\}.\end{aligned} \tag{30}$$

C. The Result of T_2^{L}

The result of T_2^{L} is the coverage probability when the typical UE is associated with the typical BS with a LoS link of distance larger than D.

$f_{\omega,2}^{\mathrm{L}}(r)$ can be derived as

$$\begin{aligned}f_{\omega_z,2}^{\mathrm{L}}(r) = &\exp\left(-\int_0^{r_1}\left(1-\Pr{}^{\mathrm{L}}(u)\right)2\pi u\lambda\mathrm{d}u\right)\\ &\times\exp\left(-\int_0^{r}\Pr{}^{\mathrm{L}}(u)2\pi u\lambda\mathrm{d}u\right)\times 0\times 2\pi r\lambda\\ &=0\ (r>D),\end{aligned} \tag{31}$$

So,

$$\begin{aligned}T_2^{\mathrm{L}} = &\int_D^{\infty}\Pr\left[\frac{P_0 g\left(A^{\mathrm{L}}\omega^{\alpha^{\mathrm{L}}}\right)^{(\epsilon-1)}}{\sigma^2+I_Z}>T\,|\mathrm{LoS}\right]\\ &\times f_{\omega_z,2}^{\mathrm{L}}(r)\mathrm{d}r=0.\end{aligned} \tag{32}$$

D. The Result of T_2^{NL}

The result of T_2^{NL} is the coverage probability when the typical UE is associated with the typical BS with a NLoS link of distance larger than D.

Lemma 3: T_2^{NL} *can be derived as*

$$\begin{aligned}T_2^{\mathrm{NL}} = &\int_D^{\infty}\exp\left(-\frac{T\sigma^2}{P_0(A^{\mathrm{NL}}\sqrt{r^2+L^2}^{\alpha^{\mathrm{NL}}})^{(\epsilon-1)}}\right)\\ &\times\mathcal{L}_{I_Z}\left(-\frac{T}{P_0(A^{\mathrm{NL}}\sqrt{r^2+L^2}^{\alpha^{\mathrm{NL}}})^{(\epsilon-1)}}\right)f_{\omega_z,2}^{\mathrm{NL}}(r)\mathrm{d}r,\end{aligned} \tag{33}$$

and the Laplace transform $\mathcal{L}_{I_Z}(s)$ *is expressed as*

$$\begin{aligned}\mathcal{L}_{I_Z}(s) = &\exp\left\{-2\pi\lambda\int_{r}^{\infty}1\right.\\ &\left.\times\int_0^{\infty}\left(f(u,x)f_{\omega_z}^{2\mathrm{NL}}(u)\,\mathrm{d}u\,|\mathrm{NLoS}\right)x\mathrm{d}x\right\}.\end{aligned} \tag{34}$$

E. The ASE and The ASE Crash Theorem

The ASE in bps/Hz/km^2 for a particular value of λ can be computed as

$$A^{\mathrm{ASE}}(\lambda,T_0) = \lambda\int_{T_0}^{\infty}\log_2(1+x)f_X(\lambda,x)\mathrm{d}x, \tag{35}$$

where T_0 is the minimum working SINR, and $f_X(\lambda,x)$ is the PDF of the SINR at the typical BS.

Since $P^{\mathrm{cov}}(\lambda,T)$ is the complementary cumulative distribution function of the SINR, $f_X(\lambda,x)$ can be expressed by

$$f_X(\lambda,x) = \frac{\partial(1-P^{\mathrm{cov}}(\lambda,x))}{\partial x}. \tag{36}$$

In this section, we explain the rational behind *the ASE Crash* in the UL of ultra dense networks (UDNs). Theorem 2 theoretically explains this phenomenon.

Theorem 2 (The ASE Crash): If $L>0$ *and* T, $T_0<+\infty$, *we have* $\lim_{\lambda\to+\infty}P^{\mathrm{cov}}(\lambda,T)=0$ *and* $\lim_{\lambda\to+\infty}A^{\mathrm{ASE}}(\lambda,T_0)=0$.

Theorem 2 states that when λ is extremely large, not only $P^{\mathrm{cov}}(\lambda,T)$ but also $A^{\mathrm{ASE}}(\lambda,T_0)$ will decrease to zero. In order to find out the fundamental reason, we need to proof that the signal-to-interference ratio (SIR) reaches one, when the BS density is extremely large. To this end, let us use the model presented in Fig. 1.

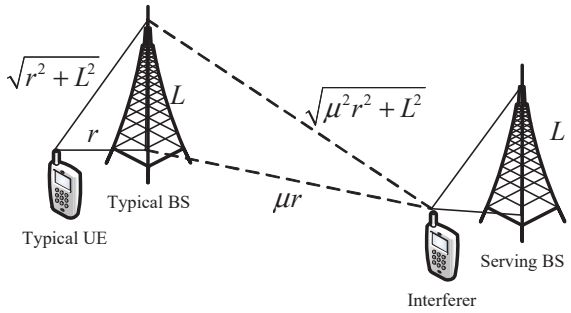

Fig. 1. Illustration of a 2-UE SCN example

As can be seen in Fig. 1, the 2D distance between the typical UE and the typical BS is r, and that between an interferer and the typical BS is μr, $(1<\mu<+\infty)$, respectively. When $\lambda\to+\infty$, we can see that $r\to 0$.

In practical SCNs [13], we also have that $L < d_1$, where d_1 is the largest distance that a LoS link can have, thus it is reasonable to assume that the signal and the stronger interferer are LoS links in this UDN model.

Based on (4), we can obtain the UE SIR ψ as

$$\psi = \frac{\left(A^{\mathrm{L}}\left(\sqrt{r^2+L^2}\right)^{\alpha^{\mathrm{L}}}\right)^{(\varepsilon-1)}}{\left(A^{\mathrm{L}}\left(\sqrt{r^2+L^2}\right)^{\alpha^{\mathrm{L}}}\right)^{\varepsilon}\left(A^{\mathrm{L}}\left(\sqrt{(\mu r)^2+L^2}\right)^{\alpha^{\mathrm{L}}}\right)^{-1}} = \left(\sqrt{\frac{1}{1+\frac{\mu^2-1}{1+\frac{L^2}{r^2}}}}\right)^{-\alpha^{\mathrm{L}}}. \tag{37}$$

Using (37), we can see that when $r \to 0$ then $\psi \to 1$ in UDNs.

Some intuitions and explanations about *the ASE Crash* are as follows:

In realistic networks, all the UEs, including the typical UE and the interferers, cannot be closer to the typical BS than L. Thus, when $\lambda \to +\infty$, both $\sqrt{r^2+L^2}$ and $\sqrt{\mu^2 r^2+L^2}$ will nearly equal to L. As a result, the path loss of the typical UE and the interferers would be the same. This leads to $\psi \to 1$, i.e., the typical BS will receive interference from every direction, and the interference power will be large enough to overwhelm the signal power. This is why both $P^{\mathrm{cov}}(\lambda, T)$ and $A^{\mathrm{ASE}}(\lambda, T_0)$ will decrease to zero when $\lambda \to +\infty$.

From (37), we can also find something interesting and important. First, the final SIR expression ψ does not depend on the FPC factor ϵ, meaning that no matter what ϵ we choose, it will not affect the SIR. Thus, the choice of ϵ does not impact/change *the ASE Crash*. Second, the BS-to-UE antenna height difference L has an impact on the SIR, and can avoid the ASE Crash, if $L = 0$. Thus, we should lower the BS antenna height straight to the UE antenna height to maximise performance. Third, α^{L} also has an impact on the SIR, and can impact/change *the ASE Crash*, except when $\sqrt{\frac{1}{1+\frac{\mu^2-1}{1+\frac{L^2}{r^2}}}} = 1$. In this case, α^{L} has no impact on the SIR, and thus cannot prevent the appearance of *the ASE Crash*.

IV. Simulations and Discussions

In this section, we investigate the network performance, and use both numerical and simulation results to establish the accuracy of our analysis. We adopt the following parameters for our 3GPP case [13], [14]: $d_1 = 300$ m, $\alpha^{\mathrm{L}} = 2.09$, $\alpha^{\mathrm{NL}} = 3.75$, $A^{\mathrm{L}} = 10^{10.38}$, $A^{\mathrm{NL}} = 10^{14.54}$, $P_0 = -76$ dBm, and $\sigma^2 = -99$ dBm.

A. Validation of the Analytical Results of $P^{\mathrm{cov}}(\lambda, T)$

For the theoretical results on the UL coverage probability studied in Section III, the results of $P^{\mathrm{cov}}(\lambda, T)$ with $\epsilon = 0.7$ in a sparse network scenario with $\lambda = 20$ BSs/km^2 and in a dense network scenario with $\lambda = 4000$ BSs/km^2 are plotted in Fig. 2.

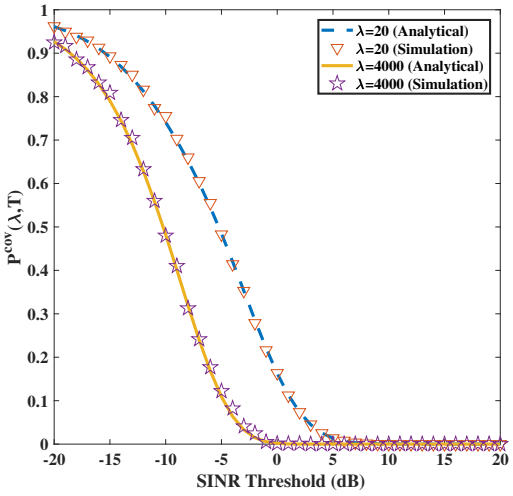

Fig. 2. $P^{\mathrm{cov}}(\lambda, T)$ vs. the SINR threshold with $\lambda = 20$ BSs/km^2 and $\lambda = 4000$ BSs/km^2

As can be observed from Fig. 2, our analytical results match the simulation results well, which indicates the accuracy of our analysis, and thus we will only use analytical results of $P^{cov}(\lambda, T)$ in our discussion hereafter.

From Fig. 2, we can draw the following observations:

- The probability of coverage SINR $> T$ increases as T decreases.
- The probability of coverage SINR $> T$ in a sparse network (small λ) is larger than that in a dense network (large λ).

Since the trend is to have more and more cells to enhance spatial reuse, it is necessary to improve the coverage probability in dense networks. Hereafter, we set $T = -3$ dB.

B. The Results of $P^{\mathrm{cov}}(\lambda, T)$ vs. λ

In Fig. 3 and Fig. 4, we show the results of $P^{\mathrm{cov}}(\lambda, T)$ with $T = -3$ dB and various BS densities. For comparison, we investigate two cases one with $L = 0$ m in Fig. 3 and another with $L = |10 - 1.5| = 8.5$ m in Fig. 4 (the BS antenna height and the UE antenna height are assumed to be 10 m and 1.5 m, respectively).

From Fig. 3, the observations are as follows:

- When the SCN is sparse, the coverage probability increases as λ increases. When the network is dense enough, the coverage probability decreases as λ increases. Thus, each curve has a maximum, and follows the conclusion in [11].
- The coverage probability with different FPC factor ϵ exhibits different trends. When the SCN is sparse, there is an optimum ϵ. However, when the network is dense enough, a lower ϵ leads to higher coverage probability. Paying special attention to the sparse SCN, the coverage probability is optimum with $\epsilon = 0.9$. Although $\epsilon = 1$ can bring a stronger signal power, the interference power is

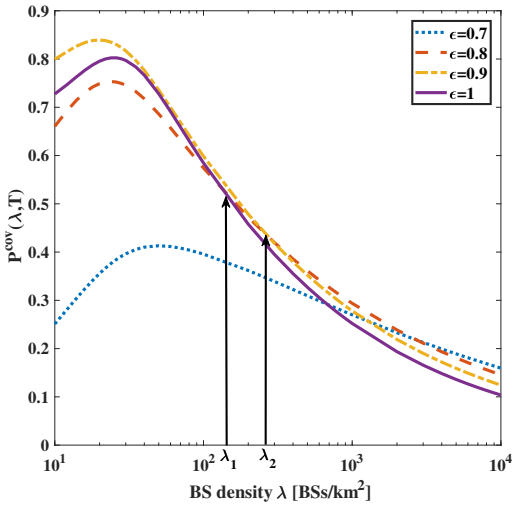

Fig. 3. $P^{\text{cov}}(\lambda, T)$ vs. λ with $T = -3$ dB and $L = 0$ m

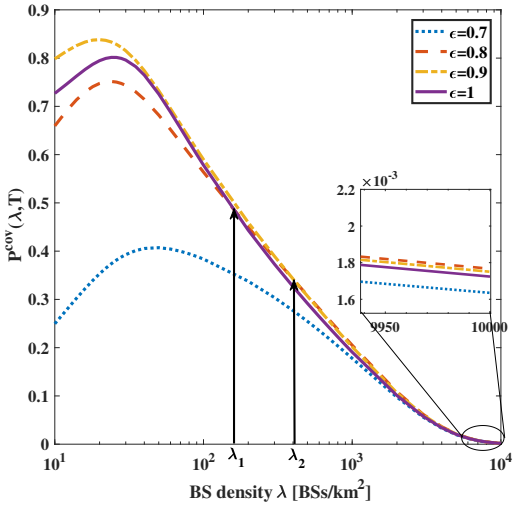

Fig. 4. $P^{\text{cov}}(\lambda, T)$ vs. λ with $T = -3$ dB and $L = 8.5$ m

still stronger than the signal one, thus leading to a smaller coverage probability.

Comparing Fig. 3 with Fig. 4, in which L adopts different values, we observe that:

- The general tendency of the coverage probability versus λ is consistent, but when $L = 8.5$ m, the coverage probability shows a more determined trajectory toward zero in the UDN regime. This trajectory matches Theorem 2, which was introduced in Section III.
- The abscissas of intersections in Fig. 4 are larger than that in Fig. 3. This means that the area occupied by the different FPC factors has changed. Interestingly, in Fig. 4, the curve with $\epsilon = 0.7$ is dominated with no intersection with the other three curves. meaning that $\epsilon = 0.7$ is not a good choice to improve coverage probability at any BS density.

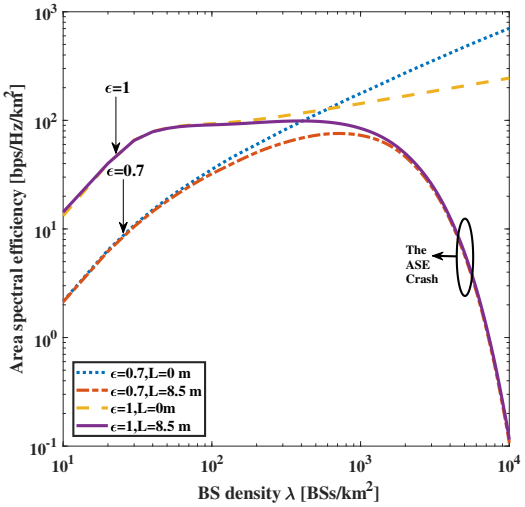

Fig. 5. $A^{\text{ASE}}(\lambda, T_0)$ vs. λ with $T = 0$ dB

- Based on Fig. 4, we suggest that when the SCN is sparse, e.g., $\lambda = 160$ BSs/km^2, $\epsilon = 0.9$ is a good choice. However, when the SCN is dense enough, although the value of $\epsilon = 0.8$ and $\epsilon = 0.9$ achieve similar performance, the former is a better choice due to the less power consumption.
- When using the same FPC factor, the highest coverage probability that a network can achieve is the same, and it is nearly achieved at the same BS density. This is because when the network is sparse, the 2D distance of the BS to the UE is much larger than 8.5 m, the BS-to-UE antenna height difference has a small effect on the downtime and even can be ignored. Furthermore, the absolute height will not change the value of the highest coverage probability.

C. The Results of $A^{ASE}(\lambda, T_0)$ vs. λ

In Fig. 5, we show the results of $A^{\text{ASE}}(\lambda, T_0)$ with $T_0 = 0$ dB based on the analytical results of $P^{\text{cov}}(\lambda, T)$. Although Fig. 5 just has 4 curves, it leads to 3 comparisons. The first and second comparisons are the ones with the same L, either $L = 0$ or $L = 8.5$ m, respectively, but different FPC factors. The third comparison is the one with different L, but the same FPC factor. The observations of each comparison are as follows:

In the first comparison, we can see that the ASE quickly increases with λ in a sparse network, i.e., $10 \sim 20$ BSs/km^2, then it exhibits a slow-down in the rate of growth. After this, the ASE continue to increase linearly with λ. The choice of best FPC factor is different from that in the coverage probability analysis. In the sparse network, a larger FPC factor always gives a better ASE performance, while in an UDN, a smaller FPC factor might be a better policy due to interference reduction.

In the second comparison, we take $\epsilon = 1$ as an example. When the SCN is sparse, i.e., $10 \sim 20$ BSs/km^2, the ASE increases linearly with λ, since the network is generally noise-limited, and thus having UEs closer to their serving BSs

improves performance. When $\lambda \in [20, 150]$ BSs/km^2, the ASE increases very slowly due to the fast decrease of coverage probability. Different from $L = 0$ m, when $L = 8.5$ m, $\epsilon = 1$ can always provide a higher ASE than $\epsilon = 0.7$.

In the last comparison, we can validate Theorem 2 in Section III:

- When $L = 8.5$ m, the ASE dramatically decreases in UDNs. Such decline of ASE in UDNs is due to *the ASE Crash* [10].
- In UDNs, e.g. $\lambda \in (3000, 10000)$ BSs/km^2, ϵ has no impact on the ASE. This means the choice of ϵ plays a negligible role in *the ASE Crash*.
- One way to avoid *the ASE Crash* is to reduce the absolute antenna height difference between a BS and a UE. Generally speaking, and according to this model, we should lower the BS antenna height, not just a few meters, but straight to the UE antenna height.

V. Conclusion

In this paper, we have shown that the absolute height difference between the BS and the UE antennas has a significant impact on the uplink performance of SCNs, including the coverage probability and the ASE. Such impact is not only quantitative but also qualitative. When the absolute height is larger than zero, the coverage probability and the ASE performance continuously decrease to zero when the BS density increases. This phenomenon is called *the ASE Crash*, which is a problem that needs to be solved in future dense network. One solution is to lower the BS antenna height to the UE antenna height. Another interesting finding is about the appropriate selection of the FPC factor. Our results reveal that the existence of the BS-to-UE antenna height difference changes the optimal operation point of the FPC compensation factor ϵ. In previous work, when absolute height equals to zero, $\epsilon = 0.7$ achieves the optimum performance in dense networks. In contrast, when considering an absolute antenna height difference, e.g. $L = 8.5$ m, we found that $\epsilon = 0.8$ can achieve a better performance. In our future work, we will analytically quantify the impact of FPC factor.

References

[1] 3GPP, "TR 36.872: Small cell enhancements for E-UTRA and E-UTRAN - Physical layer aspects," Dec. 2013.

[2] X. Ge, S. Tu, T. Han, Q. Li, and G. Mao, "Energy efficiency of small cell backhaul networks based on Gauss-Markov mobile models," *IET Networks*, vol. 4, no. 2, pp. 158–167, Mar. 2015.

[3] M. Ding, D. López-Pérez, H. Claussen, and M. A. Kaafar, "On the fundamental characteristics of ultra-dense small cell networks," *arXiv: 1710.05297 [cs.NI]*, [Online]. Available: https: //arxiv.org/abs/1710.05297. Oct. 2017.

[4] J. G. Andrews, F. Baccelli, and R. K. Ganti, "A tractable approach to coverage and rate in cellular networks," *IEEE Transactions on Communications*, vol. 59, no. 11, pp. 3122–3134, Nov. 2011.

[5] T. D. Novlan, H. S. Dhillon, and J. G. Andrews, "Analytical modeling of uplink cellular networks," *IEEE Transactions on Wireless Communications*, vol. 12, no. 6, pp. 2669–2679, Jun. 2013.

[6] B. Yu, L. Yang, H. Ishii, and S. Mukherjee, "Dynamic TDD support in macrocell-assisted small cell architecture," *IEEE Journal on Selected Areas in Communications*, vol. 33, no. 6, pp. 1201–1213, Jun. 2015.

[7] R. Mao and G. Mao, "Road traffic density estimation in vehicular networks," in *2013 IEEE Wireless Communications and Networking Conference (WCNC)*, Apr. 2013, pp. 4653–4658.

[8] S. Singh, X. Zhang, and J. G. Andrews, "Joint rate and SINR coverage analysis for decoupled uplink-downlink biased cell associations in HetNets," *IEEE Transactions on Wireless Communications*, vol. 14, no. 10, pp. 5360–5373, Oct. 2015.

[9] T. Bai and R. W. Heath, "Coverage and rate analysis for millimeter-wave cellular networks," *IEEE Transactions on Wireless Communications*, vol. 14, no. 2, pp. 1100–1114, Feb. 2015.

[10] M. Ding and D. López-Pérez, "Performance impact of base station antenna heights in dense cellular networks," *IEEE Transactions on Wireless Communications*, vol. 16, no. 12, pp. 8147–8161, Dec. 2017.

[11] T. Ding, M. Ding, G. Mao, Z. Lin, D. López-Pérez, and A. Y. Zomaya, "Uplink performance analysis of dense cellular networks with LoS and NLoS transmissions," *IEEE Transactions on Wireless Communications*, vol. 16, no. 4, pp. 2601–2613, Apr. 2017.

[12] M. Ding, D. López-Pérez, G. Mao, P. Wang, and Z. Lin, "Will the area spectral efficiency monotonically grow as small cells go dense?" in *2015 IEEE Global Communications Conference (GLOBECOM)*, Dec. 2015, pp. 1–7.

[13] 3GPP, "TR 36.828(v11.0.0): Further enhancements to LTE Time Division Duplex for Downlink-Uplink interference management and traffic adaptation," Jun. 2012.

[14] G. Mao, B. D. O. Anderson, and B. Fidan, "WSN06-4: Online calibration of path loss exponent in wireless sensor networks," in *IEEE Globecom 2006*, Nov. 2006, pp. 1–6.